Journal of Cluster Science
https://doi.org/10.1007/s10876-019-01586-9

ORIGINAL PAPER

Formation of Rhodochrosite by *Haloferax alexandrinus* GUSF-1

Sanika Naik-Samant[1,2] · Irene Furtado[1]

Received: 14 January 2019

Abstract
Bacterially mediated Mn(II) oxidation and reduction are reported from different econiches. With increase in manganese concentration in coastal regions due to anthropogenic activities, we envisage the interaction of halophilic microbes with the metal. As Haloarchaea, the extremely halophilic archaea, dominate the coastal intertidal crude salt production regions, we selected the *Haloferax alexandrinus* GUSF-1, an isolate from a salt pan of Goa, India to unveil the involvement of haloarchaea in Mn(II) conversions. Our study is a first report indicating the formation of rhodochrosite by the haloarchaeon *Haloferax alexandrinus* GUSF-1, during its growth with sodium acetate, wherein Mn(II) is accumulated intracellularly with the formation of extracellular dark brown MnO_2 that turned pinkish brown as the culture attained its stationary phase. The XRD, TEM and SEM–EDX analysis exhibited, nanometer sized electron dense regions, with cubic shaped particles characteristic to that of the mineral rhodochrosite. This biogenic formation of nano sized rhodochrosite is cost effective in comparison to that formed by oxygenic eubacteria and anoxygenic hyperthermophilic archaea, Haloarchaeon *Haloferax alexandrinus* GUSF-1, therefore attracts commercial prospect.

Keywords Haloarchaea · *Haloferax alexandrinus* GUSF-1 · Bioconversion · Mn(II) · Rhodochrosite · Microbial nanotechnology

Introduction

Manganese (III, IV) oxide minerals are abundantly distributed in terrestrial and marine environments. These oxide minerals serve as a major source for bioavailable manganese and are strongest naturally occurring oxidizing agents next to oxygen, known in the environment [1]. The oxidation of soluble Mn(II) is predominantly carried out in freshwater and marine habitats by bacteria, namely, *Bacillus* sp. strain SG-1, *Leptothrix discophora* strain SS-1 and *Pseudomonas putida* strains MnB1 and GB-1 [2–5] and in terrestrial habitats such as stratified soils by bacteria belonging to genera *Escherichia, Agromyces, Cellulomonas, Cupriavidus, Microbacterium, Ralstonia,* and *Variovorax* [6], by converting soluble Mn(II) to Mn(III/IV) oxides under harsh environmental conditions by encrusting themselves within them [7]. Biogenic formation of Mn(III, IV) oxide and oxyhydroxide mediated through bacteria is much faster than abiotic catalysis on mineral surfaces or in aqueous solution [1, 8]. Moreover, manganese oxides, carbonates and silicates are found singly or in combination as a major or minor component, in more than hundred naturally occurring minerals [9]. In recent times, Mn dioxide nanoparticles (MnO_2 NPs) are gaining importance in fabrication of biomedical sensors either singly or in association with carbon nanofibers (CNFs) [10]. MnO_2 NPs synthesized through co-precipitation method are evaluated as additives for fuel efficiency [11]. Further, manganese oxide grafted on to Fe_3O_4 nanoparticles are reported to exhibit technologically properties of both magnetic as well as catalytic properties [12]. Alternatively, most biogenic manganese oxides are important Mn oxide phases in the environment resulting in nanoparticulate materials [13, 14].

Estuarine saltpans are located alongside the estuary that serve as sinks of metal ions such as Fe(II)/Fe(III), Mn(II), Pb(II), Ni(II) originating from transportation of ore, ship building activities and industrial effluents [15]. The dominant microbial forms in these environment are the

✉ Irene Furtado
ijfurtado@unigoa.ac.in

[1] Department of Microbiology, Goa University, Taleigao Plateau, Goa 403206, India

[2] Present Address: Department of Biotechnology, Goa University, Taleigao Plateau, Goa 403206, India

Published online: 13 May 2019

haloarchaea which essentially require high concentration of NaCl (> 15%) for their growth [16]. Studies pertaining to these members of archaea carrying out biogenic oxidation of manganese ion, still remain to be unexplored. In recent times, however, haloarchaea besides being known for their high metal tolerance, are reported for its ability to adsorb Mn(II) ions from saline waters [17]. Hence, in the present study we investigated the role of haloarchaea from a estuarine saltpan in oxidation of Mn(II) in a saline milieu, using a representative isolate, the haloarchaeon *Haloferax alexandrinus* GUSF-1.

Materials and Methods

Haloarchaeal Culture

Haloferax alexandrinus GUSF-1 (GenBank accession no. KF796625) was routinely cultured and maintained at room temperature (22–28 °C) on agar slopes of NTYE medium [18].

Growth of *Haloferax alexandrinus* GUSF-1 in Presence of $MnCl_2 \cdot 6H_2O$

Four days old *Haloferax alexandrinus* GUSF-1(5% v/v) was inoculated into 500 mL flasks containing 200 mL of sterile NaCl acetate synthetic medium (NASM), consisting of (g L^{-1}): $MgSO_4 \cdot 7H_2O$ (20), NaCl (200), $MgCl_2 \cdot 6H_2O$ (13), $CaCl_2 \cdot 4H_2O$ (1), KCl (4), $NaHCO_3$ (0.2), NH_4Cl (2), $FeCl_3 \cdot 6H_2O$ (0.005), KH_2PO_4 (0.5), pH 7.0 adjusted with 1 N KOH. After adding separately sterilized sodium acetate to 0.2% final concentration, and filter sterilized Mn(II) as $MnCl_2 \cdot 6H_2O$ solution to 1 mM, the flask was incubated under static conditions at room temperature (30 °C) for 16 days. Additionally, flasks without Mn(II)/culture were maintained as control under identical incubation conditions. Aliquots of culture broth were withdrawn every 24 h and checked for absorbance A_{600} nm by UV–Vis spectrophotometer (UV2401 Shimadzu-Japan) and for concentration of Mn by atomic absorption spectrophotometer (AAS). The brown Mn-oxides formed which interfered with actual absorbance of growing culture were removed by addition of 200 µM ascorbate (1:1 v/v). In another set of flask, 10 µM of Cu(II) ions ($CuCl_2$) were added to the NASM medium containing Mn(II) ions to determine the effect on Mn(II) oxidation. Appropriate control flasks were maintained only with Mn(II) ion/without culture in the NASM.

Estimation of Manganese Oxide by Leucoberbelin Blue Assay (LBB)

Formation of Mn-oxide during growth of *Haloferax alexandrinus* GUSF-1 in NASM containing Mn(II) was analyzed colorimetrically with LBB assay [19] by adding a aliquot of 0.1 mL cell free culture broth to 1 mL of 0.04% leucoberbelin blue prepared in 45 mM acetic acid and kept standing for 1 h, at room temperature. The absorbance of blue color developed from oxidation of leucoberbelin blue was read at A_{620} nm. Absorption profile of $KMnO_4$ at A_{620} was plotted to obtain a linear relationship where 40 µM $KMnO_4$ corresponded to 100 µM MnO_2 equivalents.

Detection of Manganese Content by Atomic Absorption Spectrophotometer (AAS)

Manganese content in the cells was determined by removing aseptically 1 mL of culture broth followed by addition of 200 µM ascorbate and centrifuging at 10,000 rpm for 10 min. The cell pellet was then digested with nitric acid (HNO_3) and sulfuric acid (H_2SO_4) (2:1v/v) and was estimated for Mn by atomic absorption spectrophotometer(AA-6300 SHIMADZU) using appropriate lamp. Manganese solution in 0.1 M nitric acid, in the range of 0–15 mg L^{-1} was used to obtain the standard graph.

Physico-Chemical Characterization of Manganese Oxide Formed During Growth of *Haloferax Alexandrinus* GUSF-1

Recovery of Manganese (III/IV) Oxide from Spent Medium

Brown colored Mn(III, IV) oxide was separated from the growth medium on the 9th day by centrifugation at 10,000 rpm for 15 min and re-suspended in deionised water. The Mn-oxide pellet was washed twice with distilled water to remove culture broth impurities. The washed pellet was emptied on a clean glass plate and dried in an oven, at 80 °C. Likewise, on 16th day of growth, pinkish brown material was recovered and dried at 80 °C, separately.

X-ray Diffraction Profiling of Biogenically Formed Oxide

The dried material of brown Mn(III, IV) oxide and the pinkish brown material were separately crushed in an agate mortar and pestle and the respective fine powder was fed separately on to a special slide with an indentation window. The excess powder was wiped off and the powder sample was pressed flat with a clean glass slide. The slide holding the sample was then placed in the sample holder of the X-ray machine and scanned from 10° to 70°. Measurement were made at 0.02°, 2θ intervals with 40 s counting time, per step using Rigaku Miniflex powder diffract meter equipped with a Ultima IV solid-state detector at a voltage of 40 kV and current of 20 mA with Cu-Kα radiation, λ = 1.5418 Å. The data obtained from X-ray diffraction

(XRD) machine was plotted and full width half maxima (FWHM) was calculated using Origin 8.0 software. The crystal size was calculated by applying the Scherer's formula

$$D = k\lambda/\beta \cos\theta \quad (1)$$

where D is the mean grain size; k is a constant; λ is the X-ray wavelength for Cu-Kα radiation; β is the FWHM of the diffraction peak in radians and θ is the diffraction angle.

Scanning Electron Microscopy with Energy Dispersive X-ray Analysis (SEM-EDX) of Biogenically Formed Oxide

To observe the association of *Haloferax alexandrinus* GUSF-1 with MnO_2, the culture grown in NASM containing 1 mM of Mn(II) was centrifuged on 9th day at 10,000 rpm for 15 min and washed with 15% NaCl to remove medium impurities. On 5th day of growth, cell pellet associated with the brown material was streaked to a thin smear on a clean glass coverslip. The dried smear was fixed with (2% v/v) gluteraldehyde prepared in 15% NaCl for 24 h, followed by a series of passages in 30, 50, 70, 90 and 100% acetone, to ensure dehydration of cells. Finally coverslips were coated with gold and mounted on to the copper stub and observed under SEM equipped with EDX (JEOL JSM-5800LV).

Further, to determine the chemical composition of final pinkish brown material, the fine powder was coated on to the copper stubs as thin layer. These stubs were then sputter coated with gold using high vacuum evaporator. The position of the stage was set in such a way that the stub was approximately 50 mm from the bottom of the sputter head. After sputtering the stub with a 10–15 nm film of gold, was placed in the sample chamber of the SEM equipped with EDX and observed.

Transmission Electron Microscopy of Biogenically Formed Oxide

The morphology of pinkish brown material was evaluated using Philips CM200 transmission electron microscope (TEM) operating at 200 kV. Samples were prepared by re-suspending the dried powdered pellet in MilliQ water. 10 µL of this suspension was coated onto 2 mm carbon coated copper grids and air dried before imaging. The diameter of mineral particles in selected micrograph was measured using Image J software.

Results

The cup shaped haloarchaeon *Haloferax alexandrinus* GUSF-1 (Fig. 1a) grew with lag of 2 days in mineral salts medium with sodium acetate as sole source of carbon and reached a maximum absorbance of 1.156 at A_{600} nm after 6 days (Fig. 1b). The culture attained a stationary phase on the 9th day. Incorporation of Mn(II) ion as $MnCl_2{\cdot}6H_2O$ in the medium reduced the lag phase of growth of culture by 1 day but extended the log phase by 2 days, with absorbance reaching a maximum of 1.44 at A_{600} nm. With the onset of the stationary phase on the 9th day, the culture flasks showed increasing deposit of a light brown colored material (Fig. 1c), not seen in un-inoculated flasks having only NASM with Mn(II) and incubated under identical conditions. Simultaneous, analysis of cell free culture broth with LBB showed presence of MnO_2 detectable as a blue colored complex and corresponding to a total of 485.5 µM of MnO_2 equivalents. The SEM analysis of wet preparation of cells with brown MnO_2 (Fig. 1d) showed that the cells were closely encrusted with their Mn oxides exhibiting EDX spectra with distinct peaks for Mn at 0.5, 3.3, 6 and 6.3 keV and for oxygen at 0.2 and 0.45 keV, respectively. The formation of MnO_2 was also verified by XRD of brown material which as seen in Fig. 2a exhibited distinct peaks of δ-MnO_2 (JCPDS card no. 18-0802) with d spacing for the respective *hkl* planes as 7.25 (001), 3.59 (002), 2.43 (006), 1.43 (119). However, the formation of brown colored deposit interfered with the monitoring of absorbance A_{600} nm and consequently its correlation to growth of *Haloferax alexandrinus* GUSF-1. Addition of 200 µM of ascorbate to the culture broth resulted in disappearance of brown deposit, permitting the monitoring of actual absorbance due to growth of the culture. Addition of 2 mM sodium azide arrested the growth of *Haloferax alexandrinus* GUSF-1 and the accumulation of the brown deposit. Accumulation of Mn(II) was also detected inside the growing cells from 2nd day onwards, reaching a quantity of 582 µM mL^{-1} by the 9th day and declined thereafter to 515 µM mL^{-1} by the 11th day with no further change. Interestingly, on the 12th day the formation of MnO_2 declined to 250 µM with no further detection of same, till the 16th day whereby the brown MnO_2 gradually turned to pinkish brown in color. Furthermore, addition of copper ions to the Mn(II) containing growth medium enhanced the oxidation of manganese as detected by LBB corresponding to 565 µM of MnO_2 equivalents with cell density at A_{600} nm to be 1.44. The pinkish brown material recovered from the culture supernatants on the 16th day, totaled to 5 mg L^{-1} dry weight. Further, the pinkish brown deposit recovered on 16th day (Fig. 2b) matched with Bragg's pattern and corroborated with the records of JCPDS card no. 7-268, featuring the distinct characteristic of $MnCO_3$, the mineral rhodochrosite, with d spacing for the respective *hkl* planes as 3.66 (012), 2.84 (104), 1.770 (018), 1.763 (116). The average grain size of mineral formed by *Haloferax alexandrinus* GUSF-1 was 25 nm, determined using Scherer's formula.

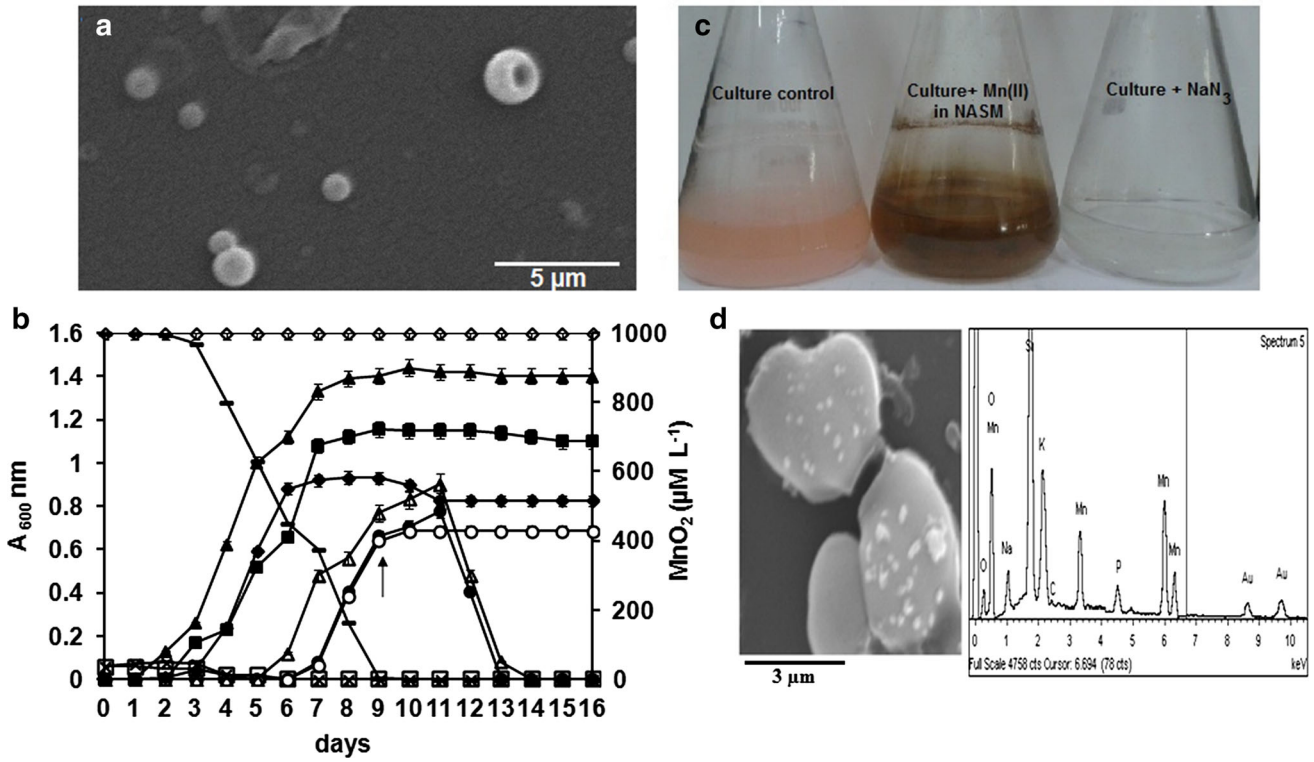

Fig. 1 **a** SEM micrograph of cup shaped *Haloferax alexandrinus* GUSF-1; **b** growth curve of *Haloferax alexandrinus* GUSF-1 in: NaCl synthetic medium containing 0.2% acetate as sole source of carbon (—■—), NASM containing 1 mM Mn(II) (—▲—), NASM containing 2 mM sodium azide (—x—), NASM containing 1 mM Mn(II) and 2 mM sodium azide (—□—), concentration of MnO_2 in culture growing in NASM with 1 mM of Mn(II) (—●—) and growing culture spiked with sodium azide on 9th day (—O—) (arrow indicates day of spiking), MnO_2 formed in growth medium incorporated with Cu(II) ions (—Δ—); Mn(II) accumulated inside growing cells over time (—♦—), concentration of Mn(II) in NASM (—◊—), concentration of Mn(II) in cell free culture broth (—); **c** flasks showing (left to right) culture grown in absence of Mn(II), Mn(IV) reduction, inhibition of Mn(II) oxidation by sodium azide in NASM; **d** SEM–EDX image of cells associated with Mn oxides

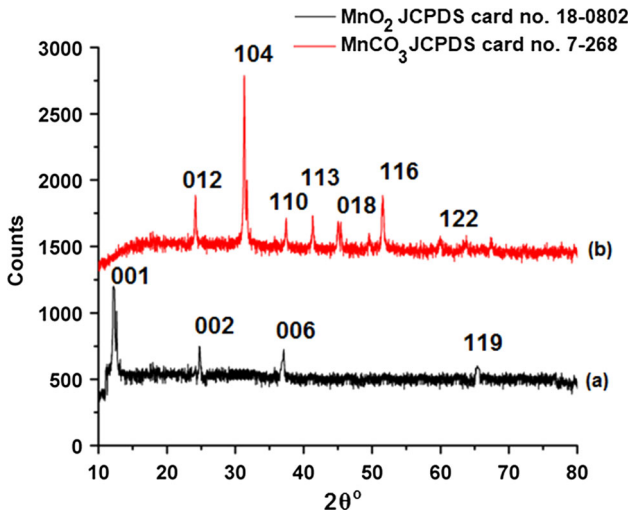

Fig. 2 X-ray diffractogram of the brown MnO_2 (a) with d values as 7.25, 3.59, 2.43, 1.43 and pinkish brown deposit $MnCO_3$ (rhodochrosite) (b) with d values as 3.66, 2.84, 1.770, 1.763 formed by *Haloferax alexandrinus* GUSF-1 recovered by centrifuging of culture broth, drying the pinkish brown pellet at 80 °C and crushing it to a fine powder

SEM profiles of the pinkish brown material, showed a crystalline surface with cubic shape (Fig. 3a). The EDX spectra displayed a peak due to Mn at 0.5, 3.3 keV and weak peaks at 5.9 keV and 6.5 keV, respectively, along with a phosphorous peak at 4.5 keV. The carbon peaks were evident at 1.2, 1.6 keV and a weak peak at 2.4 keV. Peaks due to oxygen were visible at 0.2 keV (Fig. 3b). The TEM micrographs revealed the presence of small electron dense particles of 18–25 nm in size (Fig. 4).

Discussion

Manganese oxidizing ability of bacteria and eukaryotes has been widely studied from marine and terrestrial environments. In this study, we attempted to investigate the manganese oxidizing ability of haloarchaeon namely, *Haloferax alexandrinus* GUSF-1 of the domain Archaea isolated previously from saltpans of Goa, India that are located alongside the Mandovi estuary which is known to be highly exposed to ferromanganese mining activities

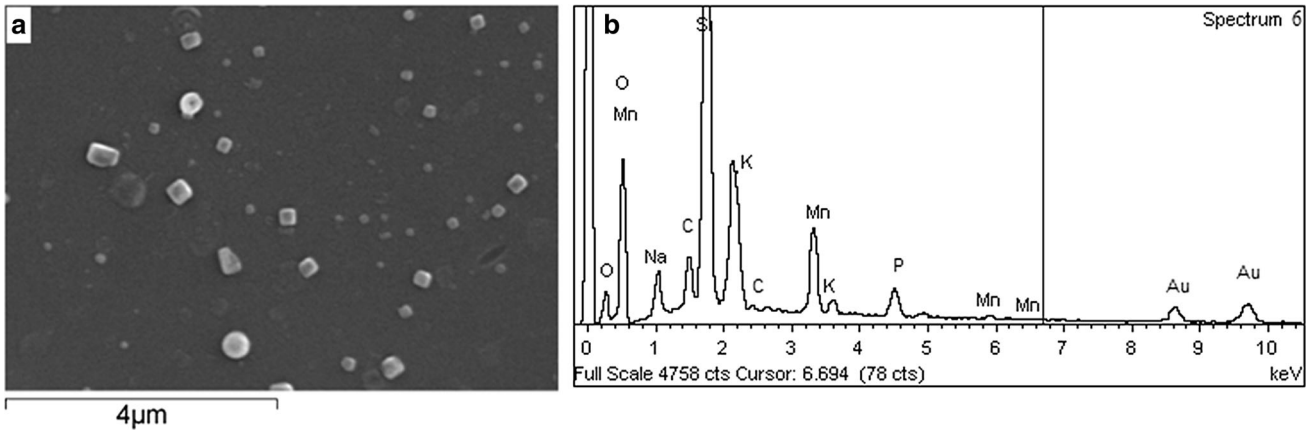

Fig. 3 Scanning electron micrograph (**a**) and energy-dispersive X-ray profile (**b**) of the pinkish brown material $MnCO_3$ (rhodochrosite) formed by *Haloferax alexandrinus* GUSF-1 coated on to the copper stubs and sputter coated with gold using high vacuum evaporator

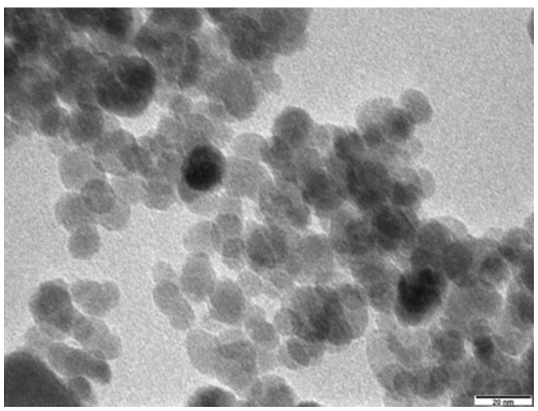

Fig. 4 Transmission electron micrographs of biogenic $MnCO_3$ (rhodochrosite) formed by *Haloferax alexandrinus* GUSF-1

[20]. Our study demonstrates not only the Mn(II) oxidizing activity of *Haloferax alexandrinus* GUSF-1 but also the formation of the mineral "rhodochrosite" by haloarchaeon. The XRD profiles and the LBB tests reveal the manganese oxidizing ability of the haloarchaeon. Mechanistically, the culture during its growth on acetate converts $MnCl_2$ [Mn(II)] → MnO_2 [Mn(IV)] → $MnCO_3$ [Mn(II)] (scheme detailed in Fig. 5). The formation of manganese oxides is purely biogenic proved from the observation that the oxidation reaction was not detected in controls with Mn(II) without the culture. The incorporation of sodium azide in the inoculated growth medium which is a metabolic inhibitor for the culture also substantiates the same showing no manganese oxidation. The conversion of Mn(II) to Mn(IV) oxide is speculated to involve Mn(II) oxidase which is an multicopper oxidase proved by the enhanced manganese oxidation on addition of Cu(II) ions to growth medium. This result also corroborates with that of *Ps. putida* GB-1 that showed increase in manganese oxidation in presence of Cu(II) ions attributed to multicopper oxidases [5, 21]. Multicopper oxidases are family of enzymes that include laccases such as ascorbate oxidases, *p*-diphenol dioxygen oxidoreductases, and other enzyme sub families [1, 22]. Moreover, occurrences of laccases are reported from halophilic euryarchaeon *Haloferax volcanii* and *Halorubrum lacusporofundi* [23]. Also, multicopper oxidases are inhibited by sodium azide hence inhibiting Mn(II) oxidizing activity and stimulated by the presence of Cu(II) ions which is also evident from our results.

Further, the growth of culture in NASM containing Mn(II) reached cell densities (A_{600} = 1.44) as compared to control without metal ion (A_{600} = 1.156) suggesting that Mn(II) or manganese oxide enhances the overall growth yield of haloarchaeal culture. This is in agreement with the hypothesis proposed by Tebo [1] and Banh [24], pointing that manganese oxide somehow enhances the cell growth by protecting it against various harmful agents such as UV-light, viral attack, scavenging of trace metals required for growth. Furthermore, the observed gradual decrease in the MnO_2 is indicative of the onset of reduction process wherein the brown material commences to turn pinkish brown color from the 12th day. The biogenic nature of this conversion is proved by spiking the growth medium with sodium azide on formation of maximum MnO_2 that arrest the metabolic activity of *Haloferax alexandrinus* GUSF-1 and thus no further reduction of MnO_2 to $MnCO_3$. The process of metal reduction under aerobic conditions has been reported previously in *Bacillus* sp. from ferromanganese nodules where it is studied that the oxygen does not interfere with microbial MnO_2 reduction [25]. This is further supported by Frankel and Bazylinski [26] stating that strict anaerobic conditions are not required for metal reducing heterotrophs, although the reduction may be most rapid under microaerophilic conditions. Also, *Acidithiobacillus* and archaea *Sulfolobus acidocaldarius* are known to reduce Fe(III) to Fe(II) while growing under aerobic conditions using sulfur as a electron donor [27]. In

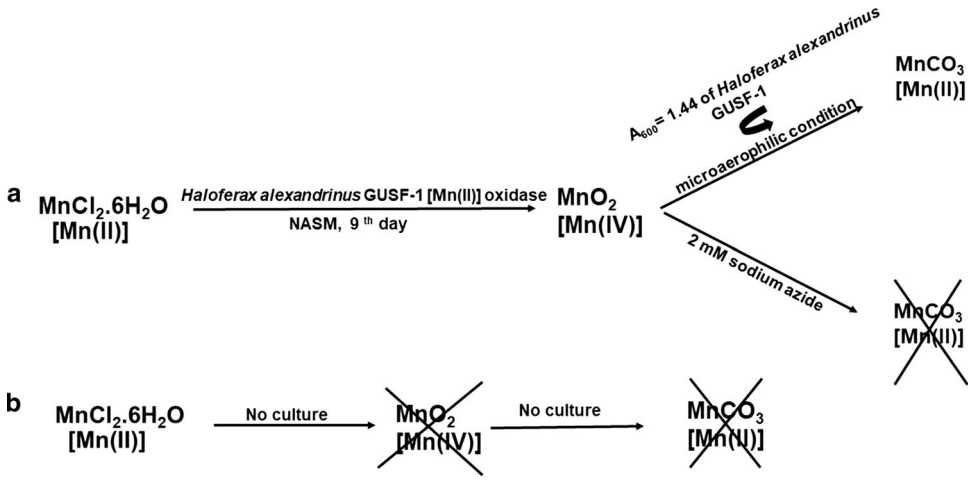

Fig. 5 Reaction scheme illustrating the synthesis of rhodochrosite ($MnCO_3$) via MnO_2 by *Haloferax alexandrinus* GUSF-1 **a** synthesis of MnO_2 and $MnCO_3$ during growth of *Haloferax alexandrinus* GUSF-1 in NASM and the inhibition of MnO_2 to $MnCO_3$ by 2 mM sodium azide, metabolic inhibitor **b** no synthesis of MnO_2 and $MnCO_3$ in absence of *Haloferax alexandrinus* GUSF-1

our study, the exact mechanism is still unclear and reflects a complex metabolic pathway. We speculate the formation of rhodochrosite and ascribe it to the presence of carbonate groups of sodium acetate contributing to carbon and to the development of microaerophilic condition, resulting due to increased cell density, particularly during the later phase of growth of culture which preferentially contribute to the formation of rhodochrosite, confirmed by XRD profiling studies. This result also corroborates with that observed in Mn(II) oxidizing bacteria isolated from terrestrial stratified soils exhibiting biogenetic reduction of Mn(III/IV) to $MnCO_3$ [6]. Although, the MnO_2 formed by *Actinobacteria* sp. in the terrestrial stratified soil is > 50 mM, it is not disclosed how much manganese is converted to $MnCO_3$. However, 76% $MnCO_3$ yield has been reported for abiotic conversion of Mn salts in presence of urea at high temperature of 80 °C [28]. Moreover, the crystalline peaks of $MnCO_3$ obtained by us resemble to mineral rhodochrosite as compared with relative intensity and positioning of peaks to the data reported by Roh et al. [29]. The clear XRD pattern distinct for δ-MnO_2 and $MnCO_3$ indicates that all the MnO_2 formed in the early stationary phase is reduced to $MnCO_3$ completely under prolong incubation in carbon rich medium. The particle size of the rhodochrosite ($MnCO_3$) in the range of 18–25 nm opens its prospects in nanostudies, particularly as chemical synthesis of nano $MnCO_3$ requires a cumbersome, sophisticated process functional at high temperatures [30]. Thus our culture is significant in producing $MnCO_3$ a compound already recognized for its application as an additive to ameliorate manganese deficient soils and increase sustainability of crops thereof [31, 32]. *Haloferax alexandrinus* GUSF-1 is previously reported for biosynthesis of silver nanoparticles [33].

In summary, *Haloferax alexandrinus* GUSF-1 is the first haloarchaeon reported for having manganese oxidizing activity and subsequently forming the mineral rhodochrosite. The formation of nanosized rhodochrosite opens its prospects for large scale production of this mineral in the world of microbial nanotechnology.

Acknowledgements Authors are indebted to Dr. M. Shyamprasad and Mr.V. Khedekar, National Institute of Oceanography, Goa, India for extending the SEM–EDX facility and to Mr. G Prabhu for helping with XRD profiling. We also thank Indian Institute of Technology, Bombay for the TEM facility.

Compliance with Ethical Standards

Conflict of interest The authors declare that they have no conflict of interest.

References

1. B. M. Tebo, H. A. Johnson, J. K. McCarthy, and A. S. Templeton (2005). *Trends. Microbiol.* **13**, 421.
2. L. G. van Waasbergen, M. Hildebrand, and B. M. Tebo (1996). *J. Bacteriol.* **178**, 3517.
3. P. L. A. M. Corstjens, J. P. M. de Vrind, T. Goosen, and E. W. de Vrind-de Jong (1997). *Geomicrobiol. J.* **14**, 91.
4. R. Caspi, B. M. Tebo, and M. G. Haygood (1998). *Appl. Environ. Microbiol.* **64**, 3549.
5. G. J. Brouwers, J. P. de Vrind, P. L. Corstjens, P. Cornelis, C. Baysse, and E. W. Jong de Vrind-de (1999). *Appl. Environ. Microbiol.* **65**, 1762.
6. W. Yang, Z. Zhang, Z. Zhang, H. Chen, J. Liu, M. Ali, F. Liu, and L. Li (2013). *PLoS ONE* **8**, e73778.
7. B. M. Tebo, J. R. Bargar, B. G. Clement, G. J. Dick, K. J. Murray, D. Parker, R. Verity, and S. M. Webb (2004). *Annu. Rev. Earth. Planet. Sci.* **32**, 287.
8. H. S. Kim, P. A. Pasten, J. F. Gaillard, and P. C. Stair (2003). *J. Am. Chem. Soc.* **125**, 14284.
9. H. L. Ehrlich, D. K. Newman, and A. Kappler *Geomicrobiology*, 5th ed (CRC, Boca Raton, 2009), pp. 401–410.
10. L. Zhang, Q. Chen, X. Han, and Q. Zhang (2018). *J. Clust. Sci.* **29**, 1089.
11. S. Jamil, S. R. Khan, B. Sultana, M. Hashmi, M. Haroon, and M. R. S. A. Janjua (2018). *J. Clust. Sci.* **29**, 1099.
12. H. J. Cui, J. W. Shi, and M. L. Fu (2012). *J. Clust. Sci.* **23**, 607.

13. J. R. Bargar, B. M. Tebo, U. Bergmann, S. M. Webb, P. Glatzel, V. Q. Chiu, and V. Mario (2005). *Am. Miner.* **90**, 143.
14. M. Villalobos, B. Toner, J. Bargar, and G. Sposito (2003). *Geochim. Cosmochim. Acta* **67**, 2649.
15. R. Alagarsamy (2006). *Estuar. Coast. Shelf Sci.* **67**, 333.
16. A. Oren (2008). *Saline Syst.* **4**, 2.
17. S. Naik and I. Furtado (2014). *Geomicrobiol. J.* **31**, 708.
18. T. M. Raghavan and I. Furtado (2000). *Bull. Environ. Contam. Toxicol.* **65**, 725.
19. Y. Lee and B. M. Tebo (1994). *Appl. Environ. Microbiol.* **60**, 2949.
20. S. M. P. Usmani (2018). *Oceanogr. Fish Open Access J.* **8**, 3.
21. Z. Zhang, Z. Zhang, H. Chen, J. Liu, C. Liu, H. Ni, C. Zhao, M. Ali, F. Liu, and L. Li (2015). *Nat. Sci. Rep.* **5**, 10895.
22. E. I. Solomon, U. M. Sundaram, and T. E. Machonkin (1996). *Chem. Rev.* **96**, 2563.
23. S. Uthandi, B. Saad, M. A. Humbard, and J. A. Maupin-Furlow (2010). *Appl. Environ. Microbiol.* **76**, 733.
24. A. Banh, V. Chavez, J. Doi, A. Nguyen, S. Hernandez, V. Ha, P. Jimenez, F. Espinoza, and H. A. Johnson (2013). *PLoS ONE* **8**, e77835.
25. R. B. Trimble and H. L. Ehrlich (1968). *Appl. Microbiol.* **16**, 695.
26. D. A. Bazylinski and R. B. Frankel in D. R. Lovley (ed.), *Environmental Microbe-Mineral Interactions* (ASM Press, Washington DC, 2000), p. 109.
27. D. R. Lovley (1991). *Microbiol. Rev.* **55**, 259.
28. E. M. Nour, S. M. Teleb, N. A. Al-Khsosy, and M. S. Refat (1997). *Synth. React. Inorg. Met. Org. Chem.* **27**, 4.
29. Y. Roh, S. V. Liu, L. Guangshan, H. Huang, T. J. Phelps, and J. Zhou (2002). *Appl. Environ. Microbiol.* **68**, 6013.
30. J. Yuan, J. Zhu, H. Bi, Z. Zhang, S. Chen, S. Liang, and X. Wang (2013). *RSC Adv.* **3**, 4400.
31. A. Ozbahce and M. Zengin (2010). *J. Plant Nutr.* **34**, 127.
32. G. V. Scaeţeanu, L. Ilie, and C. Calin (2013). *CSIJ* **3**, 247.
33. S. Patil, J. Fernandes, R. Tangasali, and I. Furtado (2014). *J. Clust. Sci.* **25**, 423.